Infection and Drug Resistance

Dovepress
Taylor & Francis Group

Open Access Full Text Article

ORIGINAL RESEARCH

Comparative Genomic Analysis of Tigecycline Resistance Development in Clinical *Acinetobacter baumannii* Isolates

Xiaoxia Li[1,*], Junnian Liu[2,*], Xinyu Zhang[1], Juan Li[3], Luhan Xuan[1], Sue Yuan[1], Jianglin Li[1], Yu Sun[1], Xuefei Du[1]

[1]Clinical Laboratory, the Fourth Affiliated Hospital of Harbin Medical University, Harbin, Heilongjiang, People's Republic of China; [2]Department of Blood Transfusion, the First Affiliated Hospital of Harbin Medical University, Harbin, Heilongjiang, People's Republic of China; [3]Department of Clinical Laboratory, Yunnan Fuwai Cardiovascular Disease Hospital, Kunming, Yunnan, People's Republic of China

*These authors contributed equally to this work

Correspondence: Xuefei Du, Clinical Laboratory, the Fourth Affiliated Hospital of Harbin Medical University, Harbin, No. 37, Yiyuan Jie, Nangang District, Harbin, Heilongjiang, 150001, People's Republic of China, Email duxuefei82@163.com; Yu Sun, Email 249292018@qq.com

Video Abstract

Point your SmartPhone at the code above. If you have a QR code reader the video abstract will appear. Or use: https://youtu.be/TLoGqOzn3Eg

Objective: This study investigated the mechanisms underlying the reduced tigecycline sensitivity of *Acinetobacter baumannii* strains isolated from infected patients during antimicrobial therapy. The goal is to provide clinical insights into the development of tigecycline resistance in *A. baumannii*, with a focus on multidrug-resistant strains commonly associated with hospital-acquired infections.

Methods: We conducted dynamic tracking of multidrug-resistant *Acinetobacter baumannii* (MDR-AB) infections in three patients to monitor changes in tigecycline sensitivity during antimicrobial therapy. From each patient, tigecycline-sensitive and -resistant *A. baumannii* strains were collected and paired into groups. A total of six strains were subjected to molecular typing and phylogenetic analysis to assess the genetic homology between the tigecycline-sensitive and -resistant strains within each group. Whole-genome sequencing and comparative genomic analysis were performed to identify single nucleotide polymorphisms and small insertions/deletions between paired strains, aiming to pinpoint mutated genes. Gene knockout experiments were conducted to validate the role of the identified genes in modulating tigecycline sensitivity and contributing to the development of tigecycline resistance in *A. baumannii*.

Results: Molecular typing and phylogenetic analysis confirmed that the tigecycline-resistant *Acinetobacter baumannii* strains isolated from each patient evolved from the initially infecting tigecycline-sensitive strains. All three patients had received tigecycline therapy before the emergence of tigecycline resistance. Notably, in one patient, resistance developed 21 days after discontinuing tigecycline treatment. Comparative genomic analysis of the paired strains revealed point mutations in the conserved domain of the trimeric autotransporter adhesin in all three groups. Additionally, a frameshift mutation in the *acrR* gene was identified in two of the three groups. To investigate the role of *acrR* in the development of tigecycline resistance, an *acrR* knockout strain was constructed. The results indicated that the *acrR* gene did not significantly impact tigecycline resistance or biofilm formation.

Conclusion: The use of tigecycline promotes the development of tigecycline resistance in *Acinetobacter baumannii*, and resistance may continue to evolve even after discontinuing tigecycline treatment. Mutations in the *ata, adeS*, and *acrR* genes may contribute to the development of tigecycline resistance in *A. baumannii*. Although gene knockout experiments in this study showed that *acrR* did not directly impact tigecycline resistance or biofilm formation, clinical isolates are influenced by a complex, multifactorial environment. Therefore, the role of *acrR* warrants further investigation.

Keywords: *Acinetobacter baumannii*, tigecycline, comparative genomics

Introduction

Acinetobacter baumannii is a prevalent Gram-negative bacillus responsible for hospital-acquired infections, capable of causing pneumonia, bacteremia, urinary tract infections, and other serious diseases.[1] As the increased use of antibiotics,

Received: 30 May 2025
Accepted: 15 August 2025
Published: 24 August 2025

particularly exposure to third-generation cephalosporins and carbapenems, has led to a rising number of reports on multidrug-resistant *A. baumannii* (MDR-AB) strains.[2] For these multidrug-resistant and even carbapenem-resistant *A. baumannii* isolates, the therapeutic options available to clinicians have become extremely limited, posing a formidable challenge to the effective clinical management of severe infections caused by this pathogen.[3]

While polymyxins have been demonstrated efficacy against MDR-AB, their clinical utility is significantly limited by substantial toxicity concerns, notably nephrotoxicity.[4] In contrast, tigecycline is widely employed for treating infections caused by MDR-AB due to its broad antibacterial spectrum, potent antimicrobial activity, and favorable safety profile.[5] Alarmingly, although tigecycline was approved in the United States in 2005, clinical isolation of *A. baumannii* strains exhibiting reduced susceptibility to tigecycline was reported as early as the following year.[6,7] Subsequently, the isolation rate of tigecycline-resistant *A. baumannii* (TRAB) has steadily risen in clinical settings, particularly, one study documented a significant rise in the isolation rate of TRAB during the COVID-19 pandemic. Moreover, findings from a separate Asia-Pacific regional study reinforced these concerns by demonstrating that, among the participating countries, *A. baumannii* isolates from China exhibited the lowest susceptibility rate to tigecycline.[8–10] It is currently accepted that the specific mechanisms contributing to reduced tigecycline susceptibility in *A. baumannii* include over-expression of efflux pump systems, production of hydrolytic enzymes, enhanced biofilm formation, and alterations in the drug target site, such as mutations in ribosomal methyltransferase genes that impair tigecycline binding; however, substantial experimental evidence has established that multidrug efflux pumps, particularly those belonging to the Resistance Nodulation cell Division (RND) family regulated by the AdeRS two-component system, play a predominant role in tigecycline resistance development in *A. baumannii*. Notably, studies have shown that mutations in the *adeS* gene frequently lead to significantly increased expression of this efflux pump system.[11,12]

The Acinetobacter trimeric autotransporter adhesin (Ata) family of proteins was first identified in *A. baumannii* ATCC 17978. Research indicates that Ata functions as a representative of the type V secretion system and is closely associated with virulence in Gram-negative bacteria, serving as an important virulence factor in *A. baumannii*, beyond this, Ata also enhances and maintains biofilm formation, which is recognized to contribute to the reinforcement of bacterial drug resistance.[13,14] The histidine kinase AdeS senses changes in the external environment, leading to the activation or inactivation of AdeR. This, in turn, regulates the expression level of the AdeABC efflux pump, thereby mediating resistance to antimicrobial agents. Transcription regulators of the AcrR family are broadly involved in regulating diverse cellular processes, including osmolarity adaptation, antibiotic synthesis, efflux pump expression, metabolic pathway enzymes, virulence, and pathogenicity; furthermore, they are also implicated in mediating multidrug resistance in bacteria through the regulation of corresponding downstream target genes.[15]

Previous studies have primarily relied on in vitro induction of resistance in tigecycline-sensitive strains, leading to findings that may deviate from the actual resistance mechanisms observed in clinical settings.[16] Given the escalating prevalence of TRAB, there is an urgent need to deepen our understanding of the mechanisms underlying tigecycline resistance development in *A. baumannii*. Such insights are critical to better guide rational clinical antimicrobial use and mitigate the emergence of bacterial resistance. This study conducted a clinical longitudinal tracking investigation of three patients. For each patient, tigecycline-sensitive strains isolated during the initial phase of antibiotic therapy were designated as reference strains, while tigecycline-resistant strains obtained during the later treatment phase served as comparator strains. And then, through whole-genome sequencing (WGS), large genomic sequence fragment closely approximating the native chromosomal structure (scaffold) was obtained. Subsequent comparative genomic analysis within each experimental group revealed inter-strain variations in scaffold architecture, single nucleotide polymorphism (SNP) variations, and small-fragment insertion/deletion (indel) mutations.

Materials and Methods

Bacterial Strains

During the period from 2016 to 2018, six MDR-AB isolates were obtained from three individual patients. Each patient contributed paired isolates: one tigecycline-susceptible strain collected at the initial phase of antimicrobial therapy and one tigecycline-resistant strain isolated following an extended course of treatment. Isolates were categorized into three

patient-specific groups: Group 1 comprised IA16004 and IA16006 (Patient 1), Group 2 included TRC15 and TR20 (Patient 2), and Group 3 consisted of TRC63 and TR21 (Patient 3). Specifically, IA16004 (Patient 1), TRC15 (Patient 2), and TRC63 (Patient 3) represent the tigecycline-susceptible baseline isolates obtained at therapy initiation, while IA16006, TR20, and TR21 correspond to the tigecycline-resistant isolates subsequently from the same patients.

In vitro Drug-Sensitivity Test

The MICs of ceftriaxone, cefepime, imipenem, gentamicin, tobramycin, ciprofloxacin, levofloxacin, and tigecycline were determined using the microbroth dilution method. Bacterial susceptibility to minocycline, amikacin, and ceftazidime was assessed via the Kirby-Bauer disk diffusion method. Quality control strains *Escherichia coli* ATCC 25922 and *Klebsiella pneumoniae* ATCC 700603 were included in all assays. Antimicrobial susceptibility interpretations followed breakpoints defined by the Clinical and Laboratory Standards Institute (CLSI M100 ED33), except for tigecycline, whose MIC values were interpreted according to US Food and Drug Administration (FDA) criteria.[17]

MLST and MLVA Typing

All collected isolates underwent initial assessment of genetic relatedness through MLST followed by MLVA. MLST was performed by amplifying seven housekeeping genes via PCR, followed by Sanger sequencing of the amplified products. The obtained sequences were submitted to the PUBMLST database (https://pubmlst.org/) for allele designation and ST determination. MLVA was conducted according to methodologies described in references.[18,19] Briefly, primers targeting variable-number tandem repeat (VNTR) loci were synthesized, and PCR-amplified products were subjected to Sanger sequencing to calculate the tandem repeat copy numbers.

Phylogenetic Tree

Phylogenetic analysis was subsequently conducted to further validate the genetic relatedness among the isolates. The 16S rDNA gene of *A. baumannii* was amplified by PCR using universal primers 27F and 1492R. The amplified products were sequenced via the Sanger method. Sequence alignment and trimming were performed with MEGA 11.0 software, and a maximum likelihood phylogenetic tree was constructed. The tree was further visualized and annotated using the iTOL online platform (https://itol.embl.de/).

Detection of RND Efflux Pump Genes

The presence of RND efflux pump genes (*adeB, adeG*, *adeJ, adeS*, *baeR, baeS*) was qualitatively analyzed using PCR coupled with agarose gel electrophoresis. Primer sequences were designed according to references.[20–23]The PCR reaction mixture (20μL total volume) contained 10μL of 2× Taq PCR Master Mix, 5μM each of forward and reverse primers, 40–100ng of template DNA, and nuclease-free water to adjust the final volume. Thermal cycling conditions were as follows: initial denaturation at 95°C for 10min; 35 cycles of denaturation at 95°C for 1min, annealing at 52°C for 30s, and extension at 72°C for 1min; followed by a final extension at 72°C for 10min. PCR products (5μL) were mixed with 1μL of nucleic acid dye and loaded onto a 2.0% agarose gel. Electrophoresis was performed at 120V for 30min, and results were visualized under visible light using a gel documentation system.

Whole-Genome Sequencing

Bacterial whole-genome sequencing was conducted using the Illumina next-generation sequencing platform. Sequencing reads were assembled with SOAP, ABySS, and SPAdes, followed by integration using CISA software. Gap closure and optimization were performed with GapCloser (version 1.12). Gene prediction included: protein-coding genes identified by GeneMarkS (version 4.17), tRNA genes predicted with tRNAscan-SE (version 1.3.1), and rRNA genes annotated via rRNAmmer (version 1.2). For small RNA (sRNA) prediction, sequences were first aligned to the Rfam database, then confirmed using cmsearch under default parameters. Functional annotation of predicted genes involved alignment of protein sequences to the GO, KEGG, COG, and NR databases. Virulence and pathogenicity were assessed using the PHI, VFDB, and ARDB databases.

Genome Comparison Analysis

For whole-genome collinearity analysis, MUMmer (Version 3.23) and LASTZ (Version 1.03.54) were used to identify regions of translocation (Trans), inversion (Inv), and translocation plus inversion (Trans+Inv). For SNP analysis, MUMmer (Version 3.23) was used to detect individual SNPs, and SNP functions were annotated based on their positional relationships and interactions with genes. SNPs in drug-resistant strains were screened using the sensitive strain's assembled genome from the same patient as the reference. For Indel analysis, LASTZ (Version 1.03.54) detected small insertions and deletions (<50bp), and Indel types were counted. Adobe Illustrator was used for figure creation.

Construction of acrR Gene Knockout Strain

High-fidelity DNA polymerase was used to amplify homologous recombination arms upstream and downstream of the *acrR* gene in the IA16004 genome. The Apramycin resistance gene *(Apr*) was amplified from the pUC57-Apr plasmid. Homologous recombination arms of *acrR* and the *Apr* gene were connected using fusion PCR to get Δ*acrR::Apr*, which was then transformed into the suicide plasmid pCVD442 to form pCVD442-Δ*acrR::Apr*. Electrotransformation introduced pCVD442-Δ*acrR::Apr* into *E. coli* β2155, creating a donor strain. Conjugation between donor strain β2155/pCVD442-Δ*acrR::Apr* and *A. baumannii* recipient strain IA16004 was performed, and Apramycin-resistant *A. baumannii* clones with integrated target plasmid were obtained on Apramycin plates, named IA16004/pCVD442-Δ*acrR::Apr*. Several IA16004/pCVD442-Δ*acrR::Apr* colonies were cultured on LB plates with 10% sucrose to form monoclonal colonies. PCR and sequencing identified clones where the *Apr* gene replaced the *acrR* gene, yielding the target strain IA16004/Δ*acrR::Apr*.

Biofilm Formation Test

As previously described,[24] with modifications. Pre-add 190μL LB broth to each well of a 96-well polystyrene plate. Prepare a 0.5McF bacterial suspension, dilute 100-fold, and add 10μL to the LB broth. Set up six replicates per sample. Incubate at 37°C for 18h. After incubation, discard the broth. Rinse each well three times with 200μL distilled water. Add 225μL of 0.1% crystal violet, let stand for 20min, rinse three times. Air-dry, add 225μL anhydrous ethanol for 20min decolorization. Transfer 125μL of the decolorized solution for absorbance measurement at 570nm using a microplate reader. Statistical analyses were performed using one-way ANOVA, with a threshold of $P < 0.05$ considered statistically significant. Significance levels are denoted as ** ($P < 0.01$) and ns (not significant, $P > 0.05$). The wild-type strain serves as the control. Perform the experiment at least three times.

Results

Clinical Information and an in vitro Drug-Sensitivity Test

This study collected three sets of *A. baumannii* strains from clinical specimens of three patients, each evolving from tigecycline-sensitive to tigecycline-resistant phenotypes during treatment. These strain pairs were categorized and designated as follows: Group 1 (IA16004 and IA16006), Group 2 (TRC15 and TR20), and Group 3 (TRC63 and TR21). The first patient was hospitalized for coronary atherosclerotic heart disease and subsequently diagnosed with bacteremia. The strains IA16004 and IA16006 were isolated sequentially from drainage fluid specimens. The second patient was admitted for acute cholecystitis, and both TRC15 and TR20 were obtained from bile specimens. The third patient received treatment for cerebrovascular disease and was clinically diagnosed with pneumonia, with strains TRC63 and TR21 isolated from sputum specimens. Immediately after collection, the three sets of experimental strains were subjected to in vitro drug-sensitivity test. Results demonstrated that all six *A. baumannii* strains exhibited multidrug-resistant phenotypes. Following intra-group comparison of the susceptibility profiles, we observed that the sensitivity to other tested antibiotics remained unchanged during the evolution of tigecycline resistance, except for levofloxacin, tigecycline, and minocycline. Among these three antibiotics with altered susceptibility, levofloxacin and minocycline showed a parallel trajectory to tigecycline, evolving from initial susceptibility or intermediate susceptibility to full resistance (Table 1), detailed breakpoint criteria are provided in Supplementary Materials Table 1.

Table 1 In vitro Drug Sensitivity Tests of Six *A. baumannii* Strains

Antibacterial Agent	Patient1		Patient2		Patient3	
	IA16004	IA16006	TRC15	TR20	TRC63	TR21
Ceftriaxone	≥64/R	≥64/R	≥64/R	≥64/R	≥64/R	≥64/R
Cefepime	≥64/R	≥64/R	≥64/R	≥64/R	≥64/R	≥64/R
Imipenem	≥16/R	≥16/R	≥16/R	≥16/R	≥16/R	≥16/R
Gentamicin	≥16/R	≥16/R	≥16/R	≥16/R	≥16/R	≥16/R
Tobramycin	≥16/R	≥16/R	≥16/	≥16/R	≥16/R	≥16/R
Ciprofloxacin	≥4/R	≥4/R	≥4/R	≥4/R	≥4/R	≥4/R
Levofloxacin	4/I	≥8/R	4/I	≥8/R	2/S	≥8/R
Tigecycline	2/S	≥8/R	2/S	≥8/R	1/S	≥8/R
Minocycline	16/S	12/R	16/S	10/R	17/S	11/R
Amikacin	6/R	6/R	6/R	6/R	6/R	6/R
Ceftazidime	6/R	6/R	6/R	6/R	6/R	6/R

Notes: Antimicrobial susceptibility interpretations followed breakpoints defined by the CLSI M100 ED33, except for tigecycline, whose MIC values were interpreted according to FDA criteria.
Abbreviations: S, susceptible; I, intermediate; R, resistant.

Timeline of Antibiotic Administration in Patients

A detailed review of the patients' medical records was conducted to delineate antibiotic administration during treatment. The analysis confirmed that all three patients had received tigecycline prior to the isolation of TRAB strains. Notably, however, strains TR20 and TR21 were isolated 10 days and 3 days after tigecycline initiation, respectively, during ongoing therapy. In contrast, for patient 1, only the tigecycline-sensitive strain IA16004 was isolated during active tigecycline treatment for *A. baumannii* infection, whereas the resistant strain IA16006 emerged 21 days post-tigecycline discontinuation. Focusing on minocycline and levofloxacin — antibiotics exhibiting concurrent susceptibility changes in this study — we observed that none of the three patients received minocycline during treatment. Interestingly, only patient 3 was administered levofloxacin during the infection management period (Figure 1).

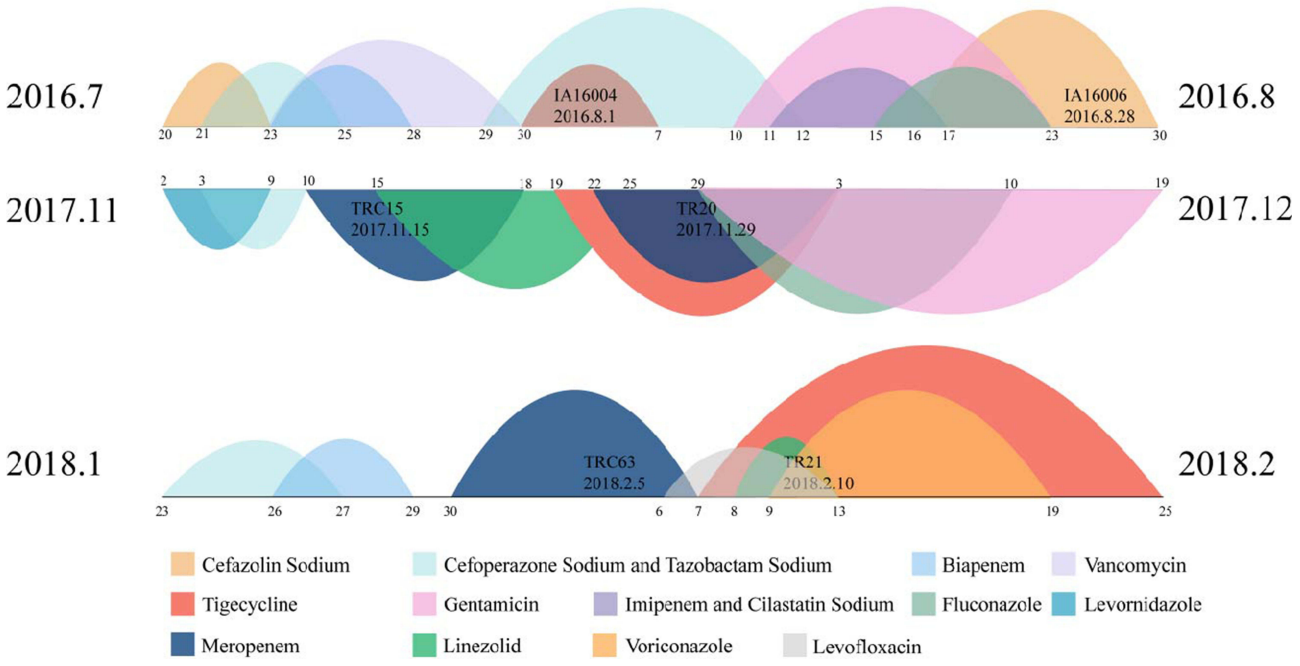

Figure 1 Antibiotic administration timeline for patients with *A. baumannii* infections during hospitalization. The start and end dates of antibiotic administration are marked by left and right boundary indicators, respectively. Numerical labels on the horizontal axis denote specific date, while distinct color codes represent individual antibiotics.

https://doi.org/10.2147/IDR.S539267

Table 2 MLVA Typing Results of *A. baumannii* in This Study

Strain	3530	3002	1988	2240	0845	0826	3468	2396
IA16004	7	7	9	3	23	20	19	41
IA16006	7	7	9	3	23	21	19	41
TRC15	9	6	9	3	21	21	9	21
TR20	9	6	9	3	18	21	11	24
TRC63	7	7	9	3	12	8	11	19
TR21	7	7	9	3	12	8	11	19

Multilocus Sequence Typing and Multiple Locus Variable-Number Tandem Repeat Analysis

Multilocus sequence typing (MLST) typing revealed that *A. baumannii* strains in Group 1 and Group 3 belonged to sequence type ST369, with a housekeeping gene sequence spectrum included *cpn60, gdhB, gltA, gpiF, gyrB, recA*, and *rpoD* (loci 2, 3, 1, 106, 3, 2, 3). Differently, strains in Group 2 were classified as ST208, which differed from ST369 solely in the *gpiF* allele, yielding an allelic profile of (loci 2, 3, 1, 97, 3, 2, 3). All six strains were identified as part of the prevalent GC2 clone, belonging to clonal complex CC92. Multiple locus variable-number tandem repeat analysis (MLVA) revealed that although differences in tandem repeat copy numbers existed among the groups, *A. baumannii* strains within each group shared identical or highly similar tandem repeat profiles, confirming their classification into same molecular genotypes (Table 2). Furthermore, combined MLST and MLVA typing results have definitively demonstrated that the TRAB strains isolated in this study evolved from their respective tigecycline-sensitive counterparts.

Phylogenetic Analysis and Carriage of RND Efflux Pump Genes

To determine the phylogenetic relationships among the six *A. baumannii* strains and assess the presence of RND efflux pump genes hypothesized to play critical roles in tigecycline resistance, we amplified their 16S rDNA via PCR and performed Sanger sequencing to construct a phylogenetic tree. The results revealed that the six strains clustered into two major clades. IA16004 and IA16006, isolated from patient 1, originated from a single branch within the first clade. The second clade further diverged into three subclades: two subclades corresponded to TRC15 and TRC20 from patient 2, while the third subclade bifurcated into two terminal branches representing TRC63 and TRC21 from patient 3. For RND efflux pump gene profiling, PCR coupled with agarose gel electrophoresis was employed to qualitatively detect six genes (*adeB, adeG, adeJ, adeS, baeR, baeS*) associated with RND efflux systems. All six genes exhibited a 100% detection rate across the six *A. baumannii* strains, irrespective of their tigecycline susceptibility status (Figure 2).

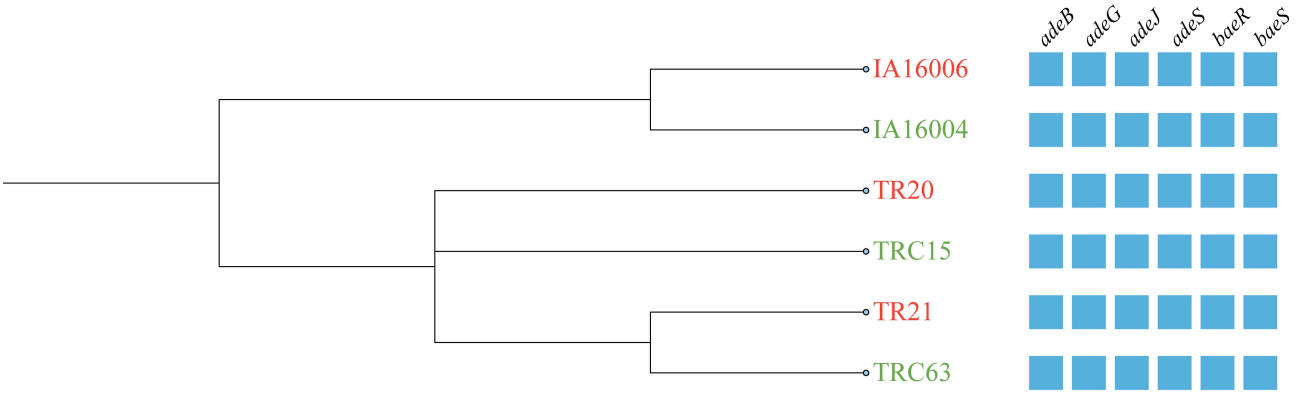

Figure 2 The phylogenetic tree of six *A. baumannii* strains. Each branch represents a strain, with resistant strains in red and sensitive ones in green. The right side of each branch shows the ST type and the carriage of efflux pump genes. A solid square means the strain carries the gene.

Genomic Characteristics of the Strains and Parallel Collinearity Analysis of the Whole Genome

Whole-genome sequencing was performed to obtain genomic data from the six *A. baumannii* strains. Within each group, tigecycline-sensitive strains were designated as reference genomes, while their resistant counterparts served as comparator genomes for alignment analysis. Post-quality control sequencing results demonstrated an average sequence identity of 97.88% between comparator and reference genomes (Table 3). Large-scale collinearity analysis revealed high genomic similarity between comparator and reference strains across all three groups. Specifically, IA16006 exhibited only three major translocation regions compared to IA16004. In contrast, TR20 showed eight distinct translocation regions relative to TRC15, while TR21 displayed four localized translocation regions compared to TRC63. Furthermore, three translocation-inversion hybrid regions were identified in Group 2, and two such regions were observed in Group 3 (Figure 3).

SNP Analysis

Comparative analysis within Group 1 revealed that the tigecycline-resistant strain IA16006 harbored eight SNPs compared to the sensitive strain IA16004. Seven of these SNPs were localized within a 6,797 bp gene, while the remaining SNP was located in an intergenic region. Among these eight SNPs, only one resulted in a nonsynonymous mutation within the conserved domain of the protein encoded by gene IA16004_GM000401. This mutation altered the 1,670th amino acid codon from AGC to AAC, leading to a substitution of serine to asparagine (Ser→Asn). This conserved domain was annotated as an Ata. Analysis of the tigecycline-resistant strain TR20 in Group 2 identified 285 SNPs relative to its sensitive counterpart TRC15, distributed across 18 genes. Within coding regions, 56 SNPs resulted in nonsynonymous mutations, including one nonsense mutation introducing a premature stop codon and three premature termination codons. Four genes with functional annotations were affected: the *XerC* gene (TRC15_GM003226), encoding a site-specific recombinase linked to mobile genetic elements, harbored four nonsynonymous mutations in its conserved domain. The Ata (TRC15_GM003573) carried two nonsynonymous mutations. One mutation at position 1,670th induced an identical serine-to-asparagine substitution observed in Group 1, while another at position 1,267th altered the codon from AGT to AAT, replacing serine with glutamine. The *adeS* gene (TRC15_GM003622), encoding a signal transduction histidine kinase, exhibited a mutation at codon 310th (GAA→AAA), substituting negatively charged glutamate with positively charged lysine. Additionally, three nonsynonymous mutations were identified in a Lysozyme family proteins domain. The remaining SNPs were associated with phage-related proteins, site-specific recombinases, putative proteins containing signal peptides, and hypothetical proteins. Only one SNP in the intergenic region occurred near a gene with known function, which is annotated as a major facilitator superfamily (MFS) permease. Finally, analysis of the tigecycline-resistant strain TR21 in Group 3

Table 3 Genomic Characteristics of *A. baumannii* in This Study

	Patient1		Patient 2		Patient 3	
	IA16004	**IA16006**	**TRC15**	**TR20**	**TRC63**	**TR21**
Genome size(bp)	4,018,155	3,949,415	4,098,462	4,118,223	4,101,443	4,100,851
Gene number	3,852	3,751	3,961	3,983	3,973	3,968
Gene total length(bp)	3,511,431	3,449,109	3,590,586	3,604,506	3,583,740	3,579,330
Gene average length(bp)	912	920	906	905	902	902
Genes of Genome (%)	87.39	87.33	87.61	87.53	87.38	87.28
GC content (%)	39	39.13	38.94	38.98	39.12	39.04
Scaffold	57	58	56	54	67	70
tRNA	63	63	63	63	63	63
5s rRNA	4	3	3	3	3	3
16s rRNA	1	1	1	1	1	1
23s rRNA	1	1	1	1	1	1
sRNA	1	1	2	2	1	1

https://doi.org/10.2147/IDR.S539267

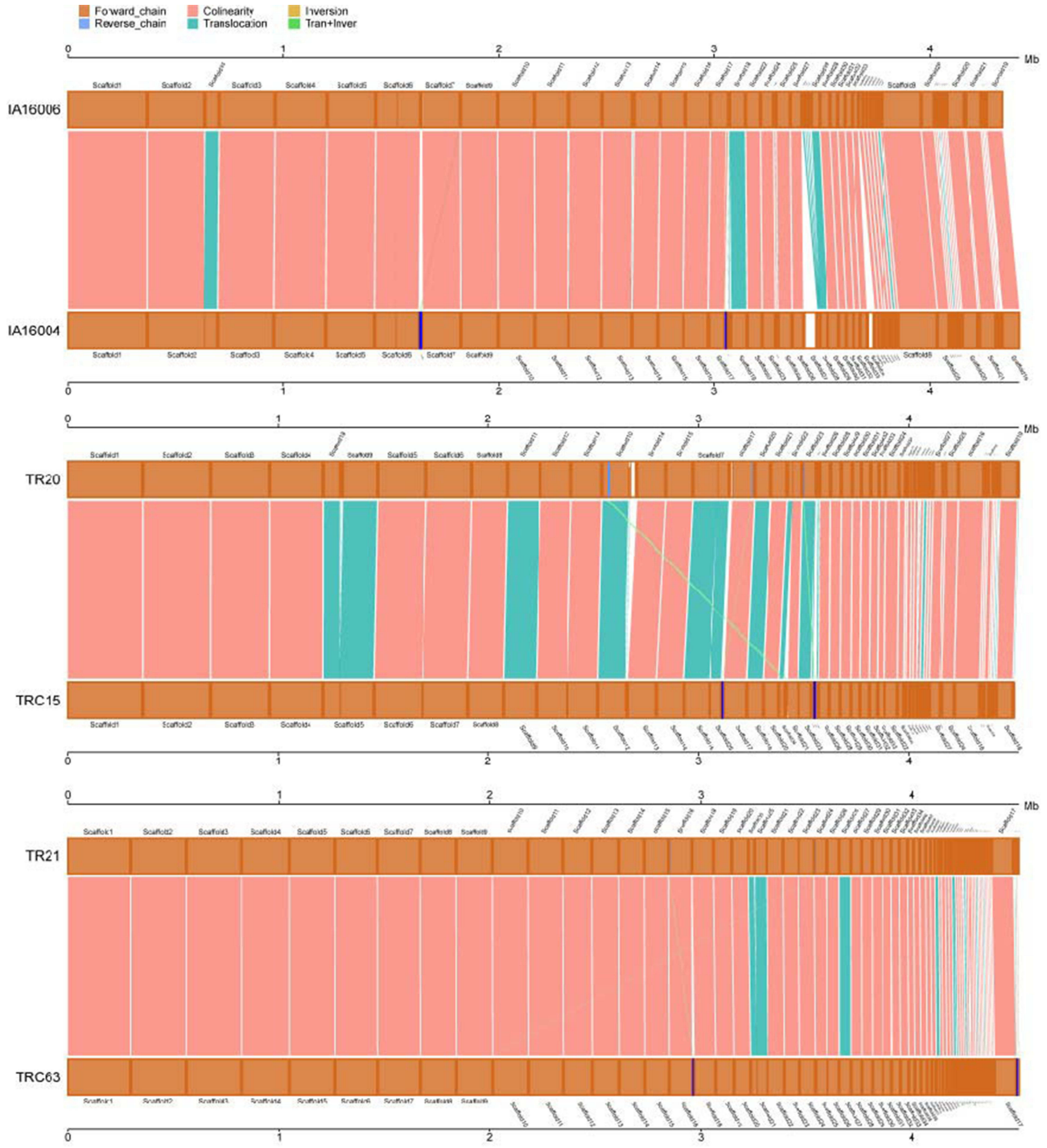

Figure 3 Whole-genome collinearity analysis of *A. baumannii* strains in this study. The upper axis represents the sequenced genomes, while the lower axis denotes the reference genome. Yellow boxes on both axes indicate forward genomic strands, and blue boxes signify reverse strands. The fill height within each box corresponds to sequence similarity (100% similarity indicated by full fill). Connecting lines between the axes are color-coded to represent alignment types: Colinearity, Translocation, Inversion, and Translocation+Inversion.

identified 92 SNPs, with 13 located in coding regions. Among these, three nonsynonymous mutations were detected. Two SNPs in the Ata were identical to those observed in the resistant strain TR20 from Group 2. A third nonsynonymous mutation occurred at position 313 of the signal transduction histidine kinase *AdeS*, altering the codon from AGG to AAG and replacing arginine with lysine (Arg→Lys). Notably, this mutation was apart just two amino acids of the *AdeS* mutation site (position 310) identified in Group 2 (Figure 4A).

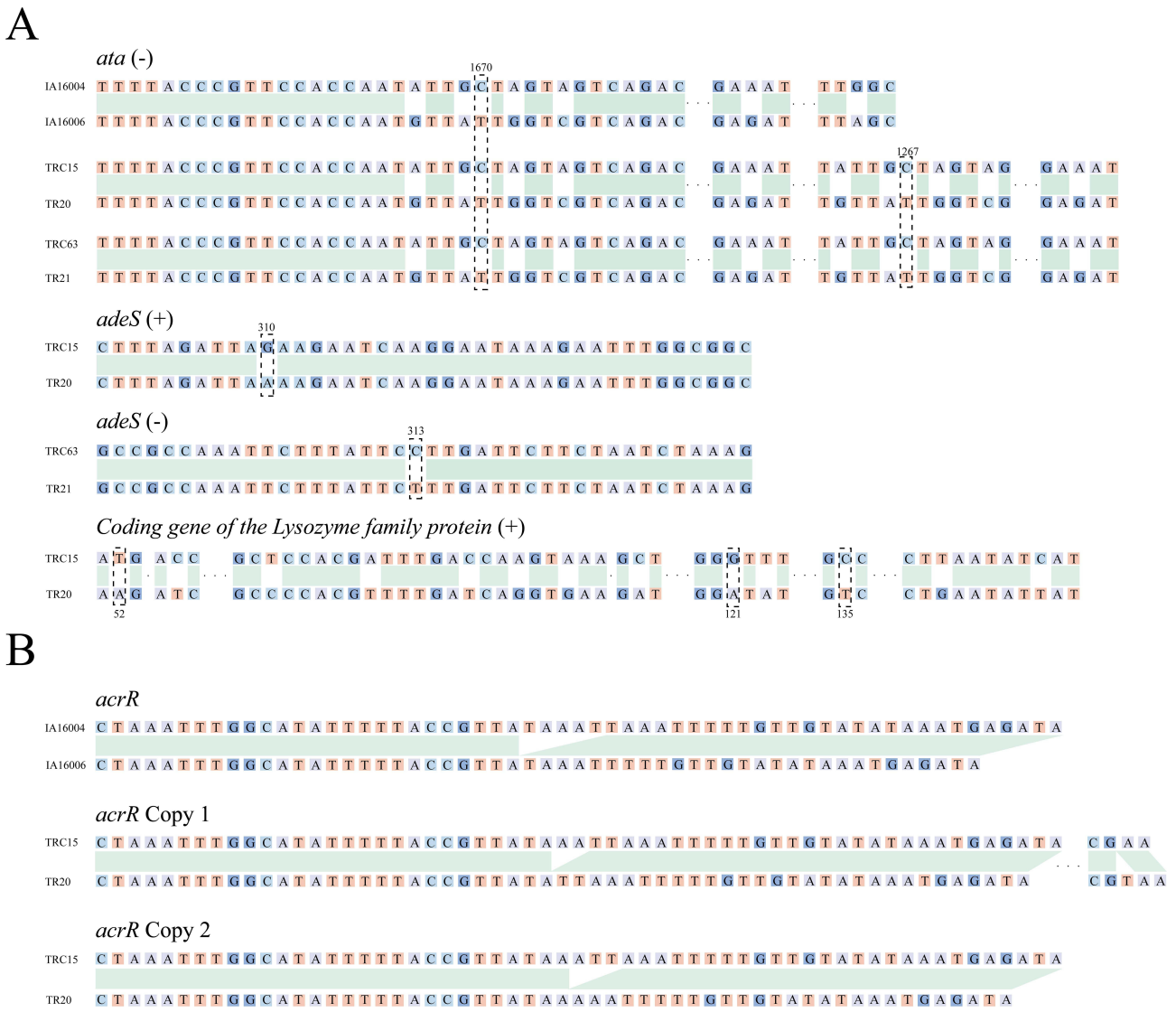

Figure 4 Comparative analysis of significant SNPs and Indels identified in functionally annotated coding regions. (**A**) SNP comparison map. Strains and mutated genes are listed on the left. Nucleotide bases are color- represented. Green shading indicates regions of sequence identity. Nonsynonymous mutation sites are marked with black dashed boxes. (**B**) Strain and gene identifiers are shown on the left. Green shading denotes regions of sequence identity.

Indel Analysis

Analysis of Group 1 Indel mutations, including two insertions and five deletions. Six Indels were located in intergenic regions, while one occurred in a coding region. The coding region Indel and two intergenic Indels were annotated to the AcrR family protein, a TetR family transcriptional regulator. AcrR proteins typically act as repressors, negatively regulating the transcription of downstream target genes. In Group 2, seven Indels were detected: three in coding regions and four in intergenic regions. Genomic annotation revealed two copies of the AcrR family protein in this group, with three Indels affecting these loci. Two mutations were located within the same gene on the antisense strand: a "T" insertion at position 316,983 and an "AA" deletion at position 317,043. The third Indel, a deletion of "ATT" occurred at position 238,623 on a separate scaffold. Group 3 exhibited seven Indels, two of which in intergenic regions were annotated to the AcrR family protein (Figure 4B).

Impact of acrR Gene Mutation on Tigecycline Drug Resistance and Biofilm Formation

To investigate the role of the *acrR* gene in modulating tigecycline susceptibility in *A. baumannii*, we constructed an *acrR* knockout strain (designated IA16004/Δ*acrR*) using the tigecycline-sensitive isolate IA16004 from patient 1. The

https://doi.org/10.2147/IDR.S539267

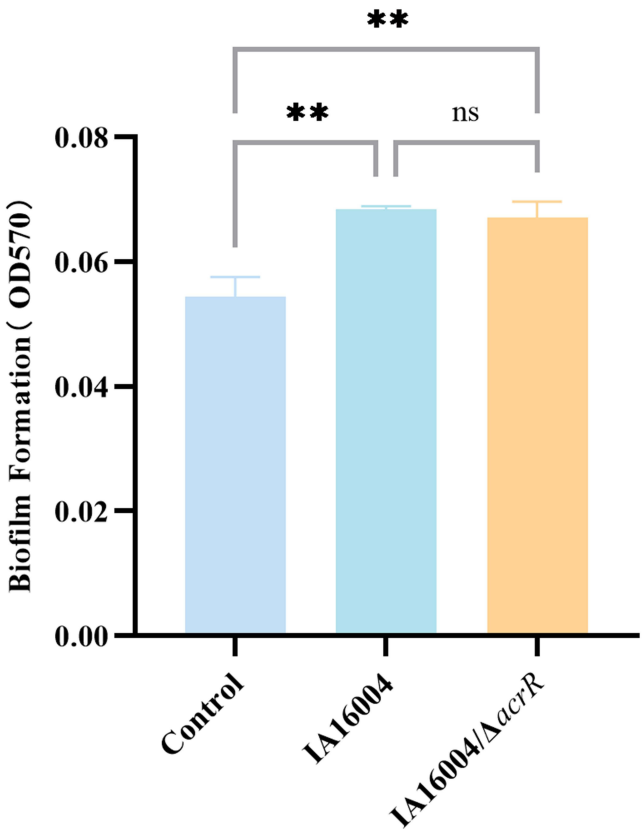

Figure 5 Biofilm formation test. The vertical axis represents biofilm biomass quantified by absorbance at OD570nm. The horizontal axis displays the control and experimental groups. **: $P < 0.01$, ns: $P > 0.05$.

microbroth dilution method was employed to assess tigecycline susceptibility in the knockout and wild-type strains. After three independent experiments, the minimum inhibitory concentration of tigecycline for IA16004/Δ*acrR* remained 0.5μg/mL, similar to that of the wild-type IA16004. Subsequently, biofilm formation assays were conducted to evaluate the impact of *acrR* deletion. The experimental results demonstrated that both IA16004 and IA16004/Δ*acrR* exhibited significant differences compared to the blank control group ($P = 0.003$ and $P = 0.0043$). However, no statistically significant difference was observed between IA16004 and IA16004/Δ*acrR* ($P = 0.7442$; Figure 5). Analysis revealed a mean value of 0.056071 ± 0.003329 (mean ± SD) for the blank control group, with the Ac value calculated as 0.0659. In contrast, the Ac values for the IA16004 and IA16004/Δ*acrR* groups were 0.068 and 0.067. According to the established criterion (Ac<A<4Ac), both IA16004 and IA16004/Δ*acrR* were classified as weakly positive (+) for biofilm formation.

Discussion

A. baumannii strains isolated in hospital settings frequently exhibit robust drug resistance, leaving clinicians with extremely limited therapeutic options.[25] In this context, polymyxins were once regarded as the last line of defense against MDR-AB infections; however, their clinical utility has been significantly constrained by substantial toxicity concerns.[26] Tigecycline, valued for its broad antimicrobial spectrum, potent antibacterial activity, and low adverse effect profile, has been more widely applied in defense against MDR-AB.[27] Nevertheless, the widespread clinical application of tigecycline—both as monotherapy and in combination regimens—has driven the rapid evolution and global dissemination of TRAB strains.[28] Consequently, elucidating the molecular mechanisms underlying tigecycline resistance in *A. baumannii* is imperative. Comprehensive research into these resistant strains is essential to decipher resistance pathways and establish effective strategies for preventing, controlling, and containing the emergence and spread of TRAB.

Current research predominantly attributes tigecycline resistance in *A. baumannii* to the overexpression and regulation of RND efflux pump genes.[29] However, a substantial body of studies has reported TRAB strains without elevated

expression of these efflux pump genes, underscoring the complexity of resistance mechanisms that likely involve multifactorial interactions rather than singular pathways.[30,31] Previous studies predominantly relied on in vitro induction of resistant strains using subinhibitory concentrations of antibiotics, followed by comparative genomic analyses of the derived mutants. However, such experimental models cannot accurately recapitulate the clinical reality of resistance development in patients, as critical parameters—including antibiotic exposure intensity, duration, and microenvironmental conditions—differ substantially between in vitro induction and actual therapeutic settings. In contrast, this study longitudinally tracked and collected paired susceptible and resistant isolates from clinical patients throughout antimicrobial therapy. This approach captures authentic clinical resistance progression trajectories, enabling comparative genomics to elucidate genuine bacterial resistance evolutionary strategies and delineate resistance emergence pathways to provide novel insights and empirical support for deciphering tigecycline resistance mechanisms in *A. baumannii*.

In vitro drug-sensitivity test revealed that, in addition to the transition from tigecycline susceptibility to resistance across all three *A. baumannii* groups, parallel evolutionary shifts were observed for minocycline and levofloxacin. Particularly, tigecycline-resistant strains from patients 2 and 3 were isolated during ongoing tigecycline therapy, whereas the resistant strain from patient 1 emerged 21 days post-discontinuation of tigecycline, suggesting potential temporal lag in phenotypic resistance development under specific clinical conditions. Importantly, despite the co-evolution of resistance to minocycline and levofloxacin in all three groups, none of the patients received minocycline during treatment, and only patient 3 had a brief history of levofloxacin exposure. This paradoxical phenomenon strongly indicates the existence of cross-resistance mechanisms linking tigecycline, minocycline, and levofloxacin, potentially mediated by shared genetic or regulatory pathways.

Summary of SNP analysis revealed nonsynonymous mutations within the conserved domain of the Ata across all three *A. baumannii* groups. Ata is a hallmark component of the type V secretion system.[13,14] Studies have established its critical role as a virulence factor in Gram-negative bacteria, particularly in *A. baumannii*.[32] Furthermore, Ata enhances and sustains biofilm formation, a process implicated in amplifying bacterial antibiotic resistance.[33] Given these dual roles in virulence and biofilm dynamics, we hypothesize that mutations in this domain may potentiate tigecycline resistance by augmenting biofilm-forming capacity. Besides, SNP analysis also identified mutations in the histidine kinase AdeS in Groups 2 and 3. Previous studies demonstrate that AdeS modulates AdeABC efflux pump expression by activating or inactivating the response regulator AdeR in response to environmental stimuli, thereby mediating antibiotic resistance.[34] A 2021 study employed comparative genomic analysis between in vitro-induced TRAB mutants and their wild-type progenitors, revealing that mutations in the *adeS* gene elevated transcriptional activity of the downstream efflux pump gene *adeB*, thereby mediating reduced tigecycline susceptibility.[35] Parallel findings by Sun et al further substantiate AdeS's role in tigecycline resistance, they utilized site-directed complementation to demonstrate that single amino acid substitutions in AdeS alone could confer decreased tigecycline susceptibility.[36] More significantly, cumulative evidence has confirmed that multiple distinct point mutations within AdeS are capable of driving tigecycline resistance in *A. baumannii*.[37,38] In this study, mutations in AdeS occurred at residues 310 and 313. Although these sites are not part of the AdeS-target gene binding interface, it has been reported that a mutation at amino acid position 310 of AdeS alters residue polarity.[39] This charge polarity reversal was hypothesized to distort the peptide's tertiary structure, impairing AdeS's ability to activate AdeR and consequently abolishing its inhibitory regulation of the AdeABC efflux pump operon, ultimately reducing tigecycline susceptibility. Therefore, the AdeS gene mutations identified in this study may also contribute to the development of tigecycline resistance in *A. baumannii*.

Following analysis of Indels in the genome, frameshift mutations in the *acrR* gene were identified in Groups 1 and 2. Multiple experiments have confirmed that mutations in *acrR* alone can upregulate the expression of the AcrAB efflux pump genes, thereby enhancing antibiotic resistance in clinical strains. Similarly, mutations in the *acrR* gene have been found to mediate the overexpression of efflux pump genes *acrA* and *acrB* in *Salmonella* Typhimurium, *K. pneumoniae*, and *Enterobacter cloacae*, resulting in increased antibiotic resistance in these bacterial strains.[15,40] Previous studies have demonstrated that *acrR* knockout in clinical *A. baumannii* strains enhances biofilm formation, motility, and invasiveness.[41] Therefore, we speculate that the frameshift mutation in the *acrR* gene may result in inactivation of its encoded AcrR protein, abolishing its repressor function. This alteration may further correlate with enhanced biofilm-forming capacity and alterations in tigecycline resistance. To validate this hypothesis, a plasmid-mediated knockout

experiment was designed to delete the AcrR coding region in the tigecycline-sensitive strain IA16004. The tigecycline susceptibility and biofilm-forming capacity of the resulting *acrR*-knockout strain were systematically evaluated. However, neither tigecycline susceptibility nor biofilm-forming capacity differed significantly between the *acrR*-knockout strain and the wild-type progenitor. Potential explanations for this unexpected outcome include: First, the *acrR* frameshift mutations detected in clinical strains may represent adaptive changes to environmental pressures unrelated to tigecycline resistance or biofilm dynamics. Second, while *acrR* mutations could theoretically contribute to these phenotypes, their effects might require synergistic interactions with other resistance determinants absent in the genetically simplified IA16004/Δ*acrR* model. Third, methodological discrepancies between the plasmid-mediated complete *acrR* deletion in our knockout strain and the natural frameshift mutations in IA16006 may yield divergent functional consequences, potentially explaining the false-negative results. But most critically, this unexpected finding precisely demonstrates the complexity of gene network regulation in the evolution of bacterial antibiotic resistance and biofilm formation, as well as the plasticity of bacterial evolutionary mechanisms. It further underscores the significance of other potential factors involving concurrent epigenetic modifications, particularly with focus on clinical strains as the research foundation.

In summary, this study employed longitudinal tracking of patients with *A. baumannii* infections, collecting three sets of strains that evolved from tigecycline-sensitive to -resistant phenotypes during hospitalization. Whole-genome sequencing and comparative genomic analyses implicate the Ata, AdeS, and *acrR* genes are may play a certain role in the development of tigecycline resistance in *A. baumannii*. The identification of these genetic determinants provides candidate biomarkers for rapid detection of resistant strains, potentially enabling early warning systems for emerging resistance, furthermore, such proactive surveillance could mitigate risks associated with excessive empirical tigecycline prescribing, thereby preventing adverse clinical outcomes. Although functional validation of *acrR* via gene knockout did not yield positive results, the limited sample size—attributable to challenges in dynamically isolating matched tigecycline-susceptible and resistant *A. baumannii* strains—remains a significant constraint. Concurrently, this deviation from established findings underscores the critical need for dynamic tracking studies using clinically relevant strains to elucidate how antibiotic resistance evolves under therapeutic pressure in real-world settings. In the Future, we will extend dynamic monitoring periods and pursue multicenter collaborations to expand sample sizes, enabling deeper mechanistic exploration and broader functional validation. Therefore, there is an urgent need for more extensive and in-depth research on TRAB, conducted as closely as possible to clinical strains to discover or refine the mechanisms of tigecycline resistance development in *A. baumannii*, and to translate these research targets into clinically applicable predictive tools for bacterial resistance. This will guide clinicians in rational antimicrobial application and reduce transmission of resistant strains.

Data Sharing Statement

The sequence data of the six Acinetobacter baumannii strains used in this study have been submitted to the NCBI database under the accession numbers (SRR16292980; SRR16292981; SRR16292982; SRR16292983; SRR16292984; SRR16292985).

Ethical Approval

This study was approved by the Medical Ethics Committee of the Fourth Affiliated Hospital of Harbin Medical University. This study was observational and did not affect the routine diagnosis and treatment of patients. We had thoroughly explained to the participants the purpose, procedures, potential benefits, and possible risks associated with this study. Informed consent was obtained from all participants prior to their inclusion in the study. The ethics review number is 2024-ethical review −09. This study was in compliance with the Declaration of Helsinki.

Acknowledgments

Xiaoxia Li and Junnian Liu are co-first authors for this study. We thank the PUBMLST website for maintaining the reliability of the data.

Funding

This research received no external funding.

Disclosure

The authors declare no conflicts of interest in this work.

References

1. Wei R, Yang X, Liu H, et al. Synthetic pseudaminic-acid-based antibacterial vaccine confers effective protection against acinetobacter baumannii Infection. *ACS Cent Sci*. 2021;7(9):1535–1542. doi:10.1021/acscentsci.1c00656
2. Romano M, Falchi F, De Gregorio E, et al. Structure-based targeting of the lipid A-modifying enzyme PmrC to contrast colistin resistance in acinetobacter baumannii. *Front Microbiol*. 2024;15:1501051. doi:10.3389/fmicb.2024.1501051
3. Rodríguez-Aguirregabiria M, Lázaro-Perona F, Cacho-Calvo JB, et al. Challenges facing two outbreaks of carbapenem-resistant acinetobacter baumannii: from cefiderocol susceptibility testing to the emergence of cefiderocol-resistant mutants. *Antibiotics*. 2024;13(8). doi:10.3390/antibiotics13080784
4. Wagenlehner F, Lucenteforte E, Pea F, et al. Systematic review on estimated rates of nephrotoxicity and neurotoxicity in patients treated with polymyxins. *Clin Microbiol Infect*. 2021. doi:10.1016/j.cmi.2020.12.009
5. Qian C, Hu P, Guo W, et al. Genome analysis of tigecycline-resistant acinetobacter baumannii reveals nosocomial lineage shifts and novel resistance mechanisms. *J Antimicrob Chemother*. 2024;79(11):2965–2974. doi:10.1093/jac/dkae314
6. Li W, DD L, Yin B, et al. Successful treatment of pyogenic ventriculitis caused by extensively drug-resistant acinetobacter baumannii with multi-route tigecycline: a case report. *World J Clin Cases*. 2021;9(3):651–658. doi:10.12998/wjcc.v9.i3.651
7. Peleg AY, Potoski BA, Rea R, et al. Acinetobacter baumannii bloodstream infection while receiving tigecycline: a cautionary report. *J Antimicrob Chemother*. 2006;59(1):128–131. doi:10.1093/jac/dkl441
8. Sun C, Yu Y, Hua X. Resistance mechanisms of tigecycline in acinetobacter baumannii. *Front Cell Infect Microbiol*. 2023;13:1141490. doi:10.3389/fcimb.2023.1141490
9. Polemis M, Mandilara G, Pappa O, et al. COVID-19 and antimicrobial resistance: data from the greek electronic system for the surveillance of antimicrobial resistance-WHONET-greece. *Life*. 2021;11(10):996. doi:10.3390/life11100996
10. Chen CH, Wu PH, Lu MC, Ho MW, Hsueh PR. Geographic patterns of carbapenem-resistant, multi-drug-resistant and difficult-to-treat acinetobacter baumannii in the asia-pacific region: results from the antimicrobial testing leadership and surveillance (ATLAS) program, 2020. *Int J Antimicrob Agents*. 2023;61(2):106707. doi:10.1016/j.ijantimicag.2022.106707
11. Lucaßen K, Müller C, Wille J, et al. Prevalence of RND efflux pump regulator variants associated with tigecycline resistance in carbapenem-resistant acinetobacter baumannii from a worldwide survey. *J Antimicrob Chemother*. 2021;76(7):1724–1730. doi:10.1093/jac/dkab079
12. Shi J, Cheng J, Liu S, Zhu Y, Zhu M. Acinetobacter baumannii: an evolving and cunning opponent. *Front Microbiol*. 2024;15:1332108. doi:10.3389/fmicb.2024.1332108
13. Pereira IL, Hartwig DD. Unveiling the role of adhesin proteins in controlling acinetobacter baumannii infections: a systematic review. *Infect Immun*. 2025;93(2):e0034824. doi:10.1128/iai.00348-24
14. Sun P, Li X, Pan C, et al. A short peptide of autotransporter ata is a promising protective antigen for vaccination against acinetobacter baumannii. *Front Immunol*. 2022;13:884555. doi:10.3389/fimmu.2022.884555
15. Bogut A, Koper P, Marczak M, Całka P. The first genomic characterization of a stable, hemin-dependent small colony variant strain of staphylococcus epidermidis isolated from a prosthetic-joint infection. *Front Microbiol*. 2023;14:1289844. doi:10.3389/fmicb.2023.1289844
16. Savari M, Ekrami A, Shoja S, Bahador A. Plasmid borne carbapenem-hydrolyzing class D β-Lactamases (CHDLs) and AdeABC efflux pump conferring carbapenem-tigecycline resistance among acinetobacter baumannii isolates harboring TnAbaRs. *Microb Pathog*. 2017;104:310–317. doi:10.1016/j.micpath.2017.01.045
17. CLSI. *Clinical and Laboratory Standards Institute*. Wayne P, USA; 2023.
18. Johnson JK, Robinson GL, Zhao L, et al. Comparison of molecular typing methods for the analyses of Acinetobacter baumannii from ICU patients. *Diagn Microbiol Infect Dis*. 2016;86(4):345–350. doi:10.1016/j.diagmicrobio.2016.08.024
19. Pourcel C, Minandri F, Hauck Y, et al. Identification of variable-number tandem-repeat (VNTR) sequences in acinetobacter baumannii and interlaboratory validation of an optimized multiple-locus VNTR analysis typing scheme. *J Clin Microbiol*. 2011;49(2):539–548. doi:10.1128/jcm.02003-10
20. Lin MF, Lin YY, Yeh HW, Lan CY. Role of the BaeSR two-component system in the regulation of Acinetobacter baumannii adeAB genes and its correlation with tigecycline susceptibility. *BMC Microbiol*. 2014;14(1):119. doi:10.1186/1471-2180-14-119
21. Meshkat Z, Salimizand H, Amini Y, et al. Detection of efflux pump genes in multiresistant Acinetobacter baumannii ST2 in Iran. *Acta Microbiol Immunol Hung*. 2021;68(2):113–120. doi:10.1556/030.2021.01314
22. Rafiei E, Shahini Shams Abadi M, Zamanzad B, Gholipour A. The frequency of efflux pump genes expression in Acinetobacter baumannii isolates from pulmonary secretions. *AMB Express*. 2022;12(1):103. doi:10.1186/s13568-022-01444-4
23. Terkuran M, Erginkaya Z, Konuray G, et al. Evaluation of antibiotic resistance and adeABC, adeR, adeS efflux pump genes among foodborne and clinical acinetobacter spp. in Türkiye. *Iran J Public Health*. 2022;51(12):2753–2763. doi:10.18502/ijph.v51i12.11466
24. Liu J, Yuan S, Xuan L, et al. Emergence of a novel sequence type carbapenem-resistant hypervirulent Klebsiella pneumoniae ST6417 harboring bla NDM-5 on the lncX3 plasmid. *Microbiol Spectr*. 2024;12(10):e0098424. doi:10.1128/spectrum.00984-24
25. Quraini MA, Jabri ZA, Sami H, et al. Exploring synergistic combinations in extended and pan-drug resistant (XDR and PDR) whole genome sequenced acinetobacter baumannii. *Microorganisms*. 2023;11(6). doi:10.3390/microorganisms11061409
26. Zhang S, Di L, Qi Y, Qian X, Wang S. Treatment of infections caused by carbapenem-resistant acinetobacter baumannii. *Front Cell Infect Microbiol*. 2024;14:1395260. doi:10.3389/fcimb.2024.1395260
27. Cui CY, He Q, Jia QL, et al. Evolutionary trajectory of the Tet(X) family: critical residue changes towards high-level tigecycline resistance. *mSystems*. 2021;6(3). doi:10.1128/mSystems.00050-21

28. Dehbanipour R, Ghalavand Z. Acinetobacter baumannii: pathogenesis, virulence factors, novel therapeutic options and mechanisms of resistance to antimicrobial agents with emphasis on tigecycline. *J Clin Pharm Ther*. 2022;47(11):1875–1884. doi:10.1111/jcpt.13787
29. Luo B, Li Z, Wang Q, Wang C. Synergistic role of biofilm-associated genes and efflux pump genes in tigecycline resistance of acinetobacter baumannii. *Med Sci Monit*. 2023;29:e940704. doi:10.12659/msm.940704
30. Zhang J, Xie J, Li H, et al. Genomic and phenotypic evolution of tigecycline-resistant acinetobacter baumannii in critically Ill patients. *Microbiol Spectr*. 2022;10(1):e0159321. doi:10.1128/spectrum.01593-21
31. Cheng J, Kesavan DK, Vasudevan A, et al. Genome and transcriptome analysis of A. Baumannii's "Transient" increase in drug resistance under tigecycline pressure. *J Glob Antimicrob Resist*. 2020;22:219–225. doi:10.1016/j.jgar.2020.02.003
32. Weidensdorfer M, Ishikawa M, Hori K, et al. The acinetobacter trimeric autotransporter adhesin Ata controls key virulence traits of acinetobacter baumannii. *Virulence*. 2019;10(1):68–81. doi:10.1080/21505594.2018.1558693
33. Bentancor LV, Camacho-Peiro A, Bozkurt-Guzel C, Pier GB, Maira-Litrán T. Identification of Ata, a multifunctional trimeric autotransporter of acinetobacter baumannii. *J Bacteriol*. 2012;194(15):3950–3960. doi:10.1128/jb.06769-11
34. Ouyang Z, Zheng F, Zhu L, et al. Proteolysis and multimerization regulate signaling along the two-component regulatory system AdeRS. *iScience*. 2021;24(5):102476. doi:10.1016/j.isci.2021.102476
35. Liu L, Shen P, Zheng B, et al. Comparative genomic analysis of 19 clinical isolates of tigecycline-resistant acinetobacter baumannii. *Front Microbiol*. 2020;11:1321. doi:10.3389/fmicb.2020.01321
36. Sun JR, Jeng WY, Perng CL, et al. Single amino acid substitution Gly186Val in AdeS restores tigecycline susceptibility of acinetobacter baumannii. *J Antimicrob Chemother*. 2016;71(6):1488–1492. doi:10.1093/jac/dkw002
37. Hornsey M, Wareham DW. Effects of in vivo emergent tigecycline resistance on the pathogenic potential of acinetobacter baumannii. *Sci Rep*. 2018;8(1):4234. doi:10.1038/s41598-018-22549-6
38. Costello SE, Gales AC, Morfin-Otero R, Jones RN, Castanheira M. Mechanisms of resistance, clonal expansion, and increasing prevalence of acinetobacter baumannii strains displaying elevated tigecycline MIC values in Latin America. *Microb Drug Resist*. 2016;22(4):253–258. doi:10.1089/mdr.2015.0168
39. Hammerstrom TG, Beabout K, Clements TP, Saxer G, Shamoo Y. Acinetobacter baumannii repeatedly evolves a hypermutator phenotype in response to tigecycline that effectively surveys evolutionary trajectories to resistance. *PLoS One*. 2015;10(10):e0140489. doi:10.1371/journal.pone.0140489
40. Gibson JS, Cobbold RN, Kyaw-Tanner MT, Heisig P, Trott DJ. Fluoroquinolone resistance mechanisms in multidrug-resistant Escherichia coli isolated from extraintestinal infections in dogs. *Vet Microbiol*. 2010;146(1–2):161–166. doi:10.1016/j.vetmic.2010.04.012
41. Maldonado J, Czarnecka B, Harmon DE, Ruiz C. The multidrug efflux pump regulator AcrR directly represses motility in Escherichia coli. *mSphere*. 2023;8(5):e0043023. doi:10.1128/msphere.00430-23